行政院國家科學委員會專題研究計畫 成果報告

利用鎳、鈀金屬化合物催化偶合反應及[2+2]環化反應之研究
研究成果報告(精簡版)

處 理 方 式 ： 本計畫可公開查詢

中 華 民 國 98 年 10 月 20 日

Bis(phenanthroimidazolyl)biphenyl derivatives as saturated blue emitters for electroluminescent devices†

Chun-Jung Kuo,[a] **Ting-Yu Li,**[a] **Chia-Chun Lien,**[a] **Charng-Hsing Liu,**[*a] **Fang-Iy Wu**[b] **and Min-Jie Huang**[b]

Blue-emitting bis(phenanthroimidazolyl)biphenyl derivatives, 4,4′-bis(1-phenyl-1*H*-phenanthro[9,10-*d*]phenanthroimidazolyl-2-yl)biphenyl (**PPIP**), 4,4′-bis(1-*p*-tolyl-1*H*-phenanthro[9,10-*d*]phenanthroimidazolyl-2-yl)biphenyl (**TPIP**) and 4,4′-bis(1-*p*-anisyl-1*H*-phenanthro[9,10-*d*]phenanthroimidazolyl-2-yl)biphenyl (**APIP**) were effectively synthesized in high yields from commercially available starting materials through a simple two-step procedure without using expensive noble-metal catalysts. These compounds showed excellent thermal properties with a very high glass-transition temperature of 197–200 °C and emitted intense blue light in solution with emission peaks at *ca.* 428 and 446 nm. By using a different hole-transporting layer, we optimized the electroluminescent efficiencies of the **PPIP**-based devices. All the **PPIP**-based devices were turned on at very low applied voltages of <3.0 V and gave pure-blue light with a Commission Internationale d'Énclairage *y*-coordinate value (CIE$_y$) ≤ 0.15. Among them, device **C** using TCTA (4,4′,4″-tris(*N*-carbazolyl)triphenylamine) as the hole-transporting layer reached a very high external quantum efficiency of 6.31% and power efficiency of 7.30 lm/W. When using **TPIP** or **APIP** as the emissive layer to replace **PPIP** in the optimal device **C**, the resulting devices also exhibited very high external quantum efficiencies of more than 5%, and highly saturated blue light can be obtained from the **TPIP**-based device with CIE$_y$ ≤ 0.10.

1. Introduction

Since the groundwork by Tang and coworkers,[1] organic light-emitting diodes (OLEDs) have been a topic of great interest for many researchers due to their application in flat-panel displays. The development of stable and highly efficient emitters of the three primary colors (red, green and blue) is crucial for OLEDs to become commercial products.[2–5] The hunt for efficient blue electroluminescence (EL) is of particular interest because it is an essential component to realize OLEDs in display as well as lighting applications. Many research groups have successfully prepared efficient blue fluorophores and OLEDs,[6–12] but efficient ones, i.e. those with a Commission Internationale d'Énclairage *y*-coordinate value (CIE$_y$) ≤ 0.15, are still relatively rare.

Although devices using s guest–host system as the emissive layer show improved EL efficiency,[6a,7c] the preparation of such doped emissive layers is usually more expensive and complicated than the fabrication of a non-doped layer during the mass-production of OLEDs. Recent works have shown that phase separation upon heating could be an important cause of degraded performances in some guest–host systems.[13] For these

reasons, many non-doped EL devices using blue host emitters as the emissive layer were prepared and some of them even exhibited extremely high external quantum efficiency (η_{ext}) (>5%).[6c,10b,11f] For example, Wu *et al.* reported a non-doped device based on a deep-blue dipyrenylbenzene emitter to reveal a high η_{ext} of 5.2% and CIE coordinates of (0.15, 0.11).[11f] By utilizing an anthracene derivative as the emissive layer, Shih *et al.* prepared another blue-emitting non-doped device having a high η_{ext} of 5.3% and excellent CIE coordinates of (0.14, 0.12).[6c] Even though these non-doped devices can achieve very high η_{ext} values, the corresponding power efficiencies (η_p) are still relatively low. This is probably due to the fact that the wide band-gap of the high-energy host emitters makes it difficult to inject charge carriers into the emissive layer from the adjacent layers. To solve this problem, Tonzola *et al.* employed an n-type oligoquinoline as the emissive layer in a blue-emitting device with high power and external quantum efficiencies of 4.3 lm/W and 6.6%, respectively, and CIE coordinates of (0.15, 0.16).[10b]

Previously, we have shown that [1,4-bis(2-(4-benzoylphenyl)-5-phenyl-1*H*-4-imidazolyl)benzene] is a blue dopant emitter for EL devices to achieve excellent CIE coordinates of (0.15, 0.12).[14] Our continuous interest in n-type imidazole derivatives as OLED emitters has prompted us to design and synthesize new compounds of this type in an attempt to improve the performance of this device. In this paper, we report the synthesis of a series of blue-emitting bis(phenanthroimidazolyl)biphenyl derivatives and their application as the host emitter in non-doped devices. These materials exhibit excellent thermal properties with glass-transition temperatures (T_g) of 197–200 °C and high photoluminescence (PL) quantum yields (50–60%). Non-doped

[a]Department of Applied Chemistry, Chia Nan University of Pharmacy and Science, Tainan, 71710, Taiwan. E-mail: liurchs@mail.chna.edu.tw; Fax: +886-6-2667319

[b]Department of Chemistry, National Tsing Hua University, Hsinchu, 30013, Taiwan

devices using a bis(phenanthroimidazolyl)biphenyl derivative, **PPIP**, as the emissive layer turned on at very low voltages of <3.0 V and exhibited pure-blue EL with $CIE_y \leq 0.15$. This optimal **PPIP**-based device can reach not only a high external quantum efficiency of 6.31% but also a high power efficiency of 7.30 lm/W. Furthermore, the power efficiency remains as high as ~5 lm/W at a practical brightness of 200 cd/m². When using **TPIP** or **APIP** as the emissive layer, the resulting devices also exhibited very high external quantum efficiencies of more than 5%, and highly saturated blue light can be obtained from the **TPIP**-based device with $CIE_y \leq 0.10$.

2. Experimental

General

Melting points (T_m), glass transition temperature (T_g) and crystallization temperature (T_c) were determined by differential scanning calorimetry (DSC) using a TA DSC Q10 instrument. Photoelectron spectra were obtained on a Riken Keiki Photoelectronic AC-2 spectrometer, while the LUMO levels were calculated based on the HOMO levels and the lowest-energy absorption edges of the UV-vis absorption spectra.[15] UV-vis absorption spectra were recorded using a Hitachi U-3300 spectrophotometer while PL and EL spectra were measured on a Hitachi F-4500 fluorescence spectrophotometer. ¹H NMR and ¹³C NMR spectra were recorded on a Bruker 200 spectrometer. High resolution mass spectra were taken with a Thermo Finnigan MAT 95 XL instrument. Elemental analyses were performed on an Elementar Vario EL III instrument. All chemicals used for electroluminescent devices were further purified by vacuum sublimation.

The EL devices were fabricated by vacuum deposition of the materials at $<5 \times 10^{-6}$ Torr onto a clean glass precoated with a layer of indium tin oxide (ITO) with a sheet resistance of 25 ohm per square. The deposition rate for organic compounds was 1–2 Å s⁻¹. The cathode was made by deposition of LiF (1.0 nm)

and then Al (100 nm) with deposition rates of 0.1 and 2–3 Å s⁻¹, respectively. For the device using poly(styrenesulfonate)-doped poly(3,4-ethylenedioxythiophene) (PEDOT) as the hole injection layer (HIL), a layer of 35-nm-thick PEDOT was deposited on the top of the ITO substrate by spin-coating from its aqueous solution, followed by baking at 120 °C for 30 min to remove the residual water. The effective area of the emitting diode was 9.00 mm². Current, voltage and light intensity measurements were made simultaneously using a Keithley 2400 source meter and a Newport 1835-C optical meter equipped with a Newport 818-ST silicon photodiode.

Synthesis of 2-(4-bromophenyl)-1-aryl-1*H*-phenanthro[9,10-*d*]imidazole derivatives 1a–1c

2-(4-Bromophenyl)-1-aryl-1*H*-phenanthro[9,10-*d*]imidazole derivatives (**1a–1c**) were prepared[16] by refluxing 9,10-phenanthrenequinone (2.0 g, 9.6 mmol), 4-bromobenzaldehyde (1.78 g, 9.6 mmol), a substituted aniline (11.5 mmol) and ammonium acetate (7.4 g, 96.1 mmol) in glacial acetic acid (40 ml) for 24 h under nitrogen atmosphere. After cooling to room temperature, the reaction mixture was poured into a methanol solution with stirring. The separated solid was filtered off, washed with methanol and dried to give the expected product in good yields. The synthetic route to the phenanthroimidazole derivatives is shown in Scheme 1. The yields and important spectral data are given below.

2-(4-Bromophenyl)-1-phenyl-1*H*-phenanthro[9,10-*d*]imidazole derivatives (1a). Yield: 3.88 g, (90%). mp = 255 °C. δ_H(200 MHz; CDCl₃; Me₄Si) 7.18 (td, *J* = 8.0, *J* = 1.1 Hz, 1H), 7.25–7.30 (m, 1H), 7.39–7.56 (m, 7H), 7.58–7.78 (m, 5H), 8.70 (d, *J* = 8.1 Hz, 1H), 8.76 (d, *J* = 8.4 Hz, 1H), 8.84 (d, *J* = 7.8 Hz, 1H); δ_C(50 MHz; CDCl₃; Me₄Si) 120.8 (d), 122.7 (d), 122.9 (s), 123.1 (d), 123.4 (s), 124.1 (d), 125.0 (d), 125.7 (d), 126.3 (d), 127.1 (s), 127.3 (d), 128.3 (s), 129.0 (d), 129.4 (s), 129.5 (s), 130.0 (d), 130.3 (d), 130.8 (d), 131.4 (d), 137.5 (s), 138.6 (s), 149.7 (s). IR (KBr): 3055,

Scheme 1 Synthesis of bis(phenanthroimidazolyl)biphenyl derivatives.

1594, 1494, 1450 cm^{-1}. HRMS (EI$^+$) Found (M$^+$): 448.0576, Calc. for C$_{27}$H$_{17}$BrN$_2$: 448.0575.

2-(4-Bromophenyl)-1-p-tolyl-1H-phenanthro[9,10-d]imidazole (1b). Yield: 3.91 g, (88%). mp = 236 °C. δ_H(200 MHz; CDCl$_3$; Me$_4$Si) 2.53 (s, 3H), 7.17–7.27 (m, 2H), 7.30–7.53 (m, 9H), 7.58–7.67 (m, 1H), 7.73 (td, J = 7.9, J = 1.0 Hz, 1H), 8.68 (d, J = 8.1 Hz, 1H), 8.74 (d, J = 8.4 Hz, 1H), 8.83 (d, J = 7.5 Hz, 1H); δ_C(50 MHz; CDCl$_3$; Me$_4$Si) 21.5 (q), 120.8 (d), 122.6 (d), 122.9 (s), 123.1 (d), 123.2 (s), 124.0 (d), 124.9 (d), 125.6 (d), 126.2 (d), 127.1 (s), 127.3 (d), 128.2 (s), 128.3 (s), 128.60 (d), 129.3 (s), 129.5 (s), 130.7 (d), 130.9 (d), 131.4 (d), 135.8 (s), 137.3 (s), 140.1 (s), 149.7 (s). IR (KBr): 3047, 2966, 1609, 1513, 1450, 1373 cm^{-1}. HRMS (EI$^+$) Found (M$^+$): 462.0729, Calc. for C$_{28}$H$_{19}$BrN$_2$: 462.0732

2-(4-Bromophenyl)-1-(4-methoxyphenyl)-1H-phenanthro[9,10-d]imidazole (1c). Yield: 3.68 g, (80%). mp = 239 °C. δ_H(200 MHz; CDCl$_3$; Me$_4$Si) 3.95 (s, 3H), 7.09 (d, J = 8.7 Hz, 2H), 7.22–7.34 (m, 1H), 7.39 (d, J = 8.7 Hz, 2H), 7.44–7.56 (m, 6H), 7.61–7.68 (m, 1H), 7.74 (td, J = 8.0, J = 1.1 Hz, 1H), 8.70 (d, J = 7.9 Hz, 1H), 8.76 (d, J = 8.4 Hz, 1H), 8.83 (d, J = 8.0 Hz, 1H); δ_C(50 MHz; CDCl$_3$; Me$_4$Si) 55.6 (q), 115.3 (d), 120.8 (d), 122.6 (d), 123.0 (s), 123.1 (d), 123.3 (s), 124.1 (d), 125.0 (d), 125.6 (d), 126.3 (d), 127.1 (s), 127.3 (d), 128.2 (s), 128.4 (s), 129.3 (s), 129.5 (s), 130.1 (d), 130.8 (d), 130.9 (s), 131.4 (d), 137.3 (s), 149.9 (s), 160.4 (s). IR (KBr): 3055, 2959, 1609, 1513, 1450, 1251, 1030 cm^{-1}. HRMS (EI$^+$) Found (M$^+$): 478.0681, Calc. for C$_{28}$H$_{19}$BrN$_2$O 478.0681

Synthesis of bis(phenanthroimidazolyl)biphenyl derivatives 2a–2c

A round-bottom flask containing compound **1a** (2.0 g, 4.45 mmol), NiCl$_2$ (0.058 g, 0.45 mmol), Zn powder (0.29 g, 4.45 mmol), KI (1.11 g, 6.68 mmol) and PPh$_3$ (0.47 g, 1.78 mmol) was purged with nitrogen three times, 20 mL of DMF was added to the flask and the mixture was stirred at 80 °C for 24 h under nitrogen. The Zn and inorganic salts were then removed by filtration of the hot reaction mixture and the residue was washed with DMF. After evaporation of the filtrate under vacuum, the residue was collected and washed with methanol and then dried in vacuum to give product **2a** (1.35 g, 82%). The product was further purified by vacuum sublimation technique at 330 °C and 3–5 × 10^{-3} Pa. The other derivatives **2b** and **2c** were prepared according to a similar procedure from compounds **1b** and **1c**, respectively. The synthetic route to for bis(phenanthroimidazolyl)biphenyl derivatives is shown in Scheme 1.The yields and important spectral data are given below.

4,4′-Bis(1-phenyl-1H-phenanthro[9,10-d]imidazole-2-yl)biphenyl (2a). Yield: 1.35 g, (82%). mp = 402 °C. δ_H(200 MHz; CDCl$_3$; Me$_4$Si) 6.73–7.79 (m, 28H), 8.72 (d, J = 8.0 Hz, 2H), 8.79 (d, J = 8.4 Hz, 2H), 8.89 (d, J = 7.9 Hz, 2H). IR (KBr): 3055, 1595, 1494, 1451 cm^{-1}. HRMS (FAB$^+$) Found (MH$^+$) 739.2861. Calc. for C$_{54}$H$_{34}$N$_4$ 738.2783. Anal. Found: C, 87.67; H, 4.68; N, 7.52. Calc. for C$_{54}$H$_{34}$N$_4$: C, 87.78; H, 4.64; N, 7.58%.

4,4′-Bis(1-p-tolyl-1H-phenanthro[9,10-d]imidazole-2-yl)biphenyl (2b). Yield: 1.37g, (80%). mp = 405 °C. δ_H(200 MHz; CDCl$_3$;

Me$_4$Si) 2.57 (s, 6H), 7.16–7.79 (m, 26H), 8.72 (d, J = 8.0 Hz, 2H), 8.78 (d, J = 8.4 Hz, 2H), 8.88 (d, J = 7.9 Hz, 2H). IR (KBr): 3055, 2915, 1605, 1513, 1450, 1376 cm^{-1}. HRMS (FAB$^+$) Found (MH$^+$) 767.3177, Calc. for C$_{56}$H$_{38}$N$_4$: 766.3096. Anal. Found: C, 87.71; H, 5.01; N, 7.34. Calc. for C$_{56}$H$_{38}$N$_4$: C, 87.70; H, 4.99; N, 7.31%.

4,4′-Bis(1-p-anisyl-1H-phenanthro[9,10-d]imidazole-2-yl)biphenyl (2c). Yield: 1.33g, (75%). mp = 403 °C. δ_H(200 MHz; CDCl$_3$; Me$_4$Si) 3.98 (s, 6H), 6.73–7.79 (m, 26H), 8.72 (d, J = 8.3 Hz, 2H), 8.78 (d, J = 8.2 Hz, 2H), 8.88 (d, J = 8.3 Hz, 2H). IR (KBr): 3062, 2959, 1601, 1509, 1458, 1249, 1031 cm^{-1}. HRMS (FAB$^+$) Found (MH$^+$) 799.3073, Calc. for C$_{56}$H$_{38}$N$_4$O$_2$: 798.2995. Anal. Found: C, 84.18; H, 4.74; N, 7.03, Calc for C$_{56}$H$_{38}$N$_4$O$_2$: C, 84.19; H, 4.79; N, 7.01%.

3. Results and discussion

3.1 Physical properties of bis(phenanthroimidazolyl)biphenyl derivatives 2

As shown in Scheme 1, the key intermediates, 2-(4-bromophenyl)-1-aryl-1H-phenanthro[9,10-d]imidazole derivatives **1a–1c**, can be easily prepared from commercially available starting materials through a simple one-step reaction in high yields (80–90%). The desired products **2a–2c** were prepared in good yields from the homo-coupling reaction of **1a–1c** at 80 °C for 24 h using NiCl$_2$/PPh$_3$ as the catalyst and Zn powder as the reducing agent. It is noteworthy that our syntheses are performed under mild reaction conditions in the presence of inexpensive metal catalysts; in addition, the overall yields for all these products are more than 60% without column chromatography purification. Therefore, the preparations of the presented bis(phenanthroimidazolyl)biphenyl derivatives are promising for large-scale production. Products **2** were fully characterized by their ^{1}H and ^{13}C NMR, high resolution mass data and elemental analysis. As shown in Fig. 1, the structure of **2a** (**PPIP**) was further confirmed by single-crystal X-ray diffraction. The central biphenyl group of PPIP adopts a coplanar configuration, and the inter-ring torsion angles between the biphenyl group and the two phenanthroimidazolyl groups are *ca.* 30°. In addition, the phenyl substituents are highly twisted about the phenanthroimidazolyl rings with dihedral angles of about 85°.

The thermal properties of the materials were examined by differential scanning calorimetry (DSC). Owing to the rigid and
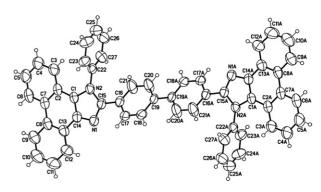

Fig. 1 X-ray structure of **PPIP**.

This journal is © The Royal Society of Chemistry 2009

J. Mater. Chem., 2009, **19**, 1865–1871 | 1867

Table 1 Physical properties of the bis(phenanthroimidazolyl)biphenyl compounds **2a–2c**

Compound	$T_m/T_g/T_c$ [a] (°C)	λ_{max}(abs) [b] (nm)	λ_{em} [b] (nm)	Quantum yield [c] (%)
2a (**PPIP**)	402/197/257	367	428, 445	58
2b (**TPIP**)	405/200/232	368	429, 446	54
2c (**APIP**)	403/ND/ND	368	429, 446	48

[a] Obtained from DSC measurement; ND: not detected. [b] Measured in dilute CH_2Cl_2 solution ($<10^{-5}$ M). [c] Measured in dilute CH_2Cl_2 solution by using 2-aminopyridine as a reference ($<10^{-5}$ M).
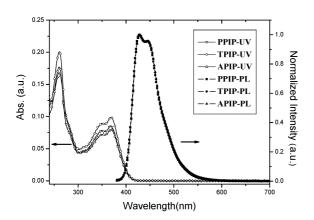

Fig. 2 The UV absorption and PL spectra of **2** in dichloromethane solution.

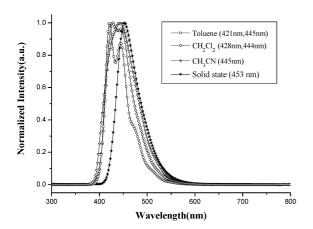**Fig. 3** The PL spectra of **PPIP** in solid state and different solvents ($<10^{-5}$ M).

non-coplanar structures (Fig. 1), the bis(phenanthroimidazolyl)biphenyl derivatives exhibited very high melting points (more than 400 °C), and in addition, distinct T_g transitions could be observed for **PPIP** and **TPIP** at 197 and 200 °C, respectively (see Table 1). Fig. 2 shows the UV-vis absorption and PL spectra of the bis(phenanthroimidazole)biphenyl derivatives **2** in dichloromethane. These materials show similar absorption spectra, with two UV absorption bands at *ca.* 260 and 370 nm. In dichloromethane solution, on the other hand, they gave an intense blue light at *ca.* 446 nm with high PL quantum yields of 48–58% by using 2-aminopyridine as a reference.[17] It is interesting to note that the emission spectra of the

bis(phenanthroimidazole)biphenyl derivatives vary with the solvent used. As shown in Fig. 3, for example, the emission peaks of **PPIP** shift towards a longer wavelength as the polarity of the solvent increases (toluene < dichloromethane < acetonitrile). This variation is likely due to the polarization-induced spectral shift.[18] In comparison with the solution PL spectra, the emission of **PPIP** in solid state is slightly red-shifted to 453 nm with a FWHM (full-width at half-maximum) of 54 nm; this small FWHM implies that there would be inconsiderable aggregation involved in its solid state.[11f]

3.2. Device characteristics using the bis(phenanthroimidazole)biphenyl derivatives as the blue host emitter

The observed intense blue emission and high T_g for the bis(phenanthroimidazole)biphenyl derivatives suggest their suitability to serve as blue host emitters in OLED applications. **PPIP** was initially selected as a host emitter for further evaluation because of its higher PL efficiency. We fabricated blue-emitting EL devices having a device configuration of ITO / HTL (hole-transporting layer) (50 nm) / **PPIP** (30 nm) / BCP (2,9-dimethyl-4,7-diphenyl-1,10-phenanthroline) (15 nm) / Alq$_3$ (tris(8-hydroxyquinolinato)aluminum) (50 nm) / LiF (1 nm) / Al (100 nm). Here we utilized three different HTLs, NPB (4,4'-bis[N-(1-naphthyl)-N-phenylamino]biphenyl), TPD (N,N'-di-m-tolyl-N,N'-diphenyl-1,1'-biphenyl-4,4'-diamine) and TCTA (4,4',4''-tris(N-carbazolyl)triphenylamine), to probe the EL properties of **PPIP**. The device structures explored in this study and the resulting performances are detailed in Table 2, and the energy levels and the chemical structures of the materials used in this study are illustrated in Fig. 4. It is clear from Fig. 5 that the three **PPIP**-based devices are turned on at a very low voltage of ≤3.0 V and then reach a maximum brightness at 12–15 V. The resulting EL spectra are displayed in the inset of Fig. 5 and very similar to the above-mentioned PL spectrum of **PPIP** in the solid state. All the three devices emitted pure-blue light with CIE$_y$ ≤ 0.15, and these values are very close to that of the blue standard for video display applications. Additionally, these **PPIP**-based devices also exhibited very stable EL spectra at a wide range of applied voltages. Taking device **B** for example, the EL spectra were unchanged as voltages increased form 6 V to the voltage required for the maximum brightness (Fig. 6).

In order to better understand the EL properties of the **PPIP**-based devices, we determined the HOMO and LUMO energy levels from the ultraviolet photoelectron spectrum and the optical band gap (calculated from the lowest-energy absorption edge of the UV-vis absorption spectrum). The HOMO/LUMO energy levels of **PPIP** are 2.8/5.7 eV. This host emitter possesses a low-lying LUMO level similar to that of a typical imidazole-based electron-transporting material TPBI (1,3,5-tris(N-phenyl-benzimidizol-2-yl)benzene).[6c,11b,f] According to the energy level diagram shown in the inset of Fig. 4, electrons could smoothly travel into **PPIP** layer by conquering small injection barriers of 0.2 eV from BCP layer which served as electron-transporting and hole-blocking layers. On the other hand, the hole injection barriers between **PPIP** and the three different HTLs are also very small (≤0.3 eV). Such small injection barriers for charge carriers may account for the observed very low turn-on voltages.

Table 2 Performance of blue-emitting OLEDs[a]

Device (HTL/EL)[b]	V_{on}[d] (V)	L (cd/m², V)	η_{ext} (%)	η_c (cd/A)	η_p (lm/W)	λ_{max} (nm)	CIE (x, y) @ 8 V
A (TPD/**PPIP**)	2.8	27680 (13.5)	4.77 (4.75)	5.92 (5.90)	4.69 (3.43)	466	(0.14, 0.15)
B (NPB/**PPIP**)	2.9	34768 (12.0)	5.41 (5.32)	6.45 (6.35)	5.13 (4.34)	464	(0.14, 0.14)
C (TCTA/**PPIP**)	3.0	18240 (15.0)	6.31 (5.89)	7.47 (6.97)	7.30 (4.94)	462	(0.15, 0.14)
D (TCTA/**TPIP**)	3.9	17300 (14.0)	5.43 (5.41)	4.69 (4.67)	2.71 (2.14)	445	(0.15, 0.09)
E (TCTA/**APIP**)	4.1	19680 (16.0)	5.26 (5.12)	6.40 (6.23)	3.84 (2.36)	464	(0.15, 0.15)
F (TCTA/**TPIP**)[c]	5.3	13710 (17.5)	5.98 (5.83)	5.76 (5.62)	2.19 (2.18)	464	(0.15, 0.10)

[a] The brightness (L), external quantum efficiency (η_{ext}), current efficiency (η_c), and power efficiency (η_p) are the maximum values of the devices; the data shown in the parentheses were taken at 200 cd/m². [b] Device configuration: ITO / HTL (50 nm) / EL (30 nm) / BCP (15 nm) / Alq (30nm) / LiF (1 nm) / Al (100 nm). [c] Using PEDOT as the hole injection layer. [d] V_{on} is defined as the voltage required for 1 cd/m².
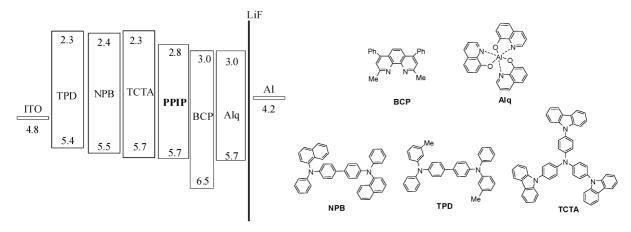

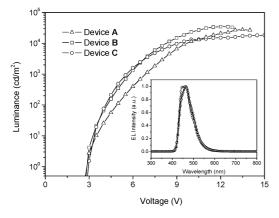**Fig. 4** Chemical structures and energy levels of the materials used in this study.

Fig. 5 Luminance vs. voltage characteristics of devices **A**–**C**. Inset: the EL spectra at 8 V.
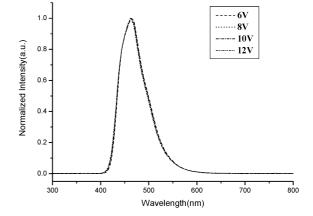

Fig. 6 The EL spectra of device **B** at various applied voltages.

As shown in Table 2 and Fig. 7, the **PPIP**-based devices exhibited very high EL efficiency. The maximum external quantum efficiency and current efficiency achieved by these devices are 4.77–6.31% and 5.92–7.47 cd/A, respectively. When using TCTA as the HTL, the resulting device **C** achieves the most efficient pure-blue light among the devices. This result could be attributed the more balanced charge-transporting properties within the emissive layer achieved by better charge injection and confinement provided by TCTA HTL. As well as having high η_{ext} and η_c values, the **PPIP**-based devices also preserve a relatively high level of power efficiency at (4.69–7.30 lm/W) because of

their low driving voltages. Although efficient non-doped OLEDs with extremely high external quantum efficiencies and excellent color purity have been reported, the corresponding peak power efficiencies are still relatively low (<4.5 lm/W).[6c,10b,11f] At a more practical brightness of 200 cd/m², the power efficiency of device **C** can still retain at a high level of *ca.* 5 lm/W (Table 2 and Fig. 7). It is noteworthy that device **C** is the first reported OLED device that emits pure-blue light with high power efficiency at practical brightness levels. Based on the results of the device optimization on HTL, we selected TCTA as the HTL to fabricate devices **D** and **E**, using **TPIP** and **APIP** as the blue host emitters,
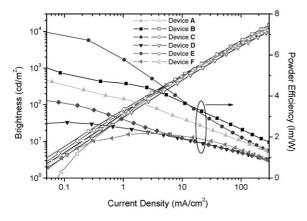
Fig. 7 Plots of brightness (empty symbols) and power efficiency (filled symbols) as a function of current density for devices **A**–**F**.
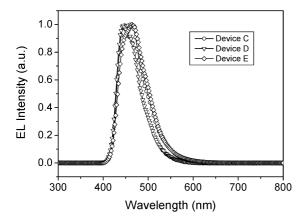

Fig. 8 The EL spectra of devices **C**–**E** at 8 V.

respectively. As presented in Table 2, the turn-on voltages of these two devices are higher than that of the corresponding **PPIP**-based device; this is probably owing to the higher-lying LUMO and HOMO energy levels (2.5–2.7 and 5.4–5.6 eV, respectively) of the host emitters used in the former, which leads to larger electron injection barriers at the host emitter–BCP interface. However, devices **D** and **E** can still achieve very high external quantum efficiency (>5%) even at 200 cd/m^2 (Table 2). The EL spectra of the devices using the three new bis(phenanthroimidazolyl)biphenyl derivatives as the emissive layer are compared in Fig. 8. The emission contribution of device **D** in the sky-blue and green spectral region is less than the other two, and hence a highly saturated blue electroluminescence with CIE coordinates of (0.15, 0.09) can be obtained from this device. In attempt to further improve the performance of device **D**, PEDOT (poly(styrenesulfonate)-doped poly(3,4-ethylenedioxythiophene))[19] was inserted between ITO and TCTA to serve as the hole-injection layer in device **F**. The peak external quantum efficiency and current efficiency of device **F** were significantly raised to 5.98% and 5.76 cd/A, respectively (Table 2). To the best of knowledge, the external quantum efficiency achieved by this device is the highest yet achieved for deep-blue OLEDs.[20,21]

4. Conclusion

We successfully synthesized three bis(phenanthroimidazolyl)biphenyl derivatives in high yields *via* convenient synthetic routes. These materials showed excellent thermal properties with very high glass-transition temperatures (around 200 °C) and an efficient blue emission at *ca.* 465 nm. The non-doped EL devices based on the three new bis(phenanthroimidazolyl)biphenyl derivatives as the emissive layer gave very high external quantum efficiency (more than 5%) even at brightness levels up to 200 cd/m^2. Among them, the **PPIP**-based device also had very high power efficiency of 7.30 lm/W because of its low driving voltage; on the other hand, the **TPIP**-based device emitted highly saturated blue light with CIE$_y$ $\leq$ 0.10 owing to the smaller emission contribution in the sky-blue and green spectral region.

References

1 C. W. Tang and S. A. Van Slyke, *Appl. Phys. Lett.*, 1987, **51**, 913.
2 *Organic Electroluminescent Materials and Devices*, ed. S. Miyata and H. S. Nalwa, Gordon and Breach, New York, 1997.
3 T. Wakimoto, H. Ochi, S. Kawami, H. Ohata, K. Nagayama, R. Murayama, H. Okuda, T. Tohma, T. Naito and H. Abiko, *J. Soc. Inf. Disp.*, 1997, **5**, 235.
4 P. E. Burrows, G. Gu, V. Bulovic, Z. Shen, S. R. Forrest and M. E. Thompson, *IEEE Trans. Electron Devices*, 1997, **44**, 1188.
5 (*a*) L. S. Hung and C. H. Chen, *Mater. Sci. Eng., R*, 2002, **39**, 143; (*b*) C. H. Chen, C. W. Tang, J. Shi and K. P. Klubek, *Macromol. Symp.*, 1998, **125**, 49.
6 (*a*) J. Shi and C. W. Tang, *Appl. Phys. Lett.*, 2002, **80**, 3201; (*b*) Y.-H. Kim, H.-C. Jeong, S.-H. Kim, K. Yang and S.-K. Kwon, *Adv. Funct. Mater.*, 2005, **15**, 1799; (*c*) P. I. Shih, C.-Y. Chuang, C.-H. Chien, E. W.-G. Diau and C.-F. Shu, *Adv. Funct. Mater.*, 2007, **17**, 3141; (*d*) Y.-Y. Lyu, J. Kwak, O. Kwon, S.-H. Lee, D. Kim, C. Lee and K. Char, *Adv. Mater.*, 2008, **20**, 2729.
7 (*a*) F.-I. Wu, C.-F. Shu, T.-T. Wang, E. W.-G. Diau, C.-H. Chien, C.-H. Chuen and Y.-T. Tao, *Synth. Met.*, 2005, **151**, 285; (*b*) F.-I. Wu, P.-I. Shih, M.-C. Yuan, A. K. Dixit, C.-F. Shu, Z.-M. Chung and E. W.-G. Diau, *J. Mater. Chem.*, 2005, **15**, 4753; (*c*) M.-T. Lee, C.-H. Liao, C.-H. Tsai and C. H. Chen, *Adv. Mater*, 2005, **17**, 2493; (*d*) Y. Duan, Y. Zhao, P. Chen, J. Li, S. Liu, F. He and Y. Ma, *Appl. Phys. Lett.*, 2006, **88**, 263503.
8 (*a*) Z. Q. Gao, Z. H. Li, P. F. Xia, M. S. Wong, K. W. Cheah and C. H. Cheng, *Adv. Funct. Mater.*, 2007, **17**, 3194; (*b*) S. Jiao, Y. Liao, X. Xu, L. Wang, G. Yu, L. Wang, Z. Su, S. Ye and Y. Liu, *Adv. Funct. Mater.*, 2008, **18**, 2335.
9 H.-T. Shih, Y.-T. Lin and C.-H. Cheng, *Adv. Mater.*, 2002, **14**, 1409.
10 (*a*) A. P. Kulkami, A. P. Gifford, C. J. Tozola and S. A. Jenekhe, *Appl. Phys. Lett.*, 2005, **86**, 061106; (*b*) C. J. Tonzola, A. P. Kukarni, A. P. Gifford, W. Kaminsky and S. A. Jenekhe, *Adv. Funct. Mater.*, 2007, **17**, 863.
11 (*a*) C.-H. C, K.-C. Wu, US Pat., 6861163, 2005; (*b*) S. Tao, Z. Peng, X. Zhang, P. Wang, C.-S. Lee and S.-T. Lee, *Adv. Funct. Mater.*, 2005, **15**, 1716; (*c*) C. Tang, F. Liu, Y.-J. Xia, L.-H. Xie, A. Wei, S.-B. Li, Q.-L. Fan and W. J. Huang, *J. Mater. Chem.*, 2006, **16**, 4074; (*d*) J. A. Mikroyannidis, L. Fenenko and C. Adachi, *J. Phys. Chem. B*, 2006, **110**, 20317; (*e*) M. Y. Lo, C. Zhen, M. Lauters, G. E. Jabbour and A. Sellinger, *J. Am. Chem. Soc.*, 2007, **129**, 5808; (*f*) K.-C. Wu, P.-J. Ku, C.-S. Lin, H.-T. Shih, F.-I. Wu, 2M.-J. Huang, J.-J. Lin, I.-C. Chen and C.-H. Cheng, *Adv. Funct. Mater.*, 2008, **18**, 67.

12 (a) T. Tominaga, A. Makiyama and T. Kohama, JP Pat., 2003059670, 2003; (b) T. Tominaga, D. Kitazawa and A. Takano, JP Pat., 2001023777, 2001.

13 (a) G. Y. Zhong, Z. Xu, S. T. Zhang, W. Huang and X. Y. Hou, *Appl. Phys. Lett.*, 2002, **81**, 1122; (b) S.-C. Chang, G. He, F.-C. Chen, T.-F. Guo and Y. Yang, *Appl. Phys. Lett.*, 2001, **79**, 2088; (c) J.-R. Gong, L.-J. Wan, S.-B. Lei, C.-L. Bai, X.-H. Zhang and S.-T. Lee, *J. Phys. Chem. B*, 2005, **109**, 1675.

14 A. Islam, C.-C. Tsou, H.-J. Hsu, W.-L. Shih, C.-H. Liu and C.-H. Cheng, *Tamkang Journal of Science and Engineering*, 2002, **5**, 69.

15 S. Janietz, D. D. C. Bradley, M. Grell, C. Giebeler, M. Inbasekaran and E. P. Woo, *Appl. Phys. Lett.*, 1998, **73**, 2453.

16 V. K. Mahesh, M. Maheswari and R. Sharma, *Can. J. Chem.*, 1985, **63**, 635.

17 G. Jones II, W. R. Jackson, C. Y. Choi and W. R. Bergmark, *J. Phys. Chem.*, 1985, **89**, 294.

18 V. Bulovic, A. Shoustikov, M. A. Baldo, E. Bose, V. G. Kozlov, M. E. Thomoson and S. R. Forrest, *Chem. Phys. Lett.*, 1998, **287**, 455.

19 T. M. Brown, J. S. Kim, R. H. Friend, F. Cacialli, R. Daik and W. J. Feast, *Appl. Phys. Lett.*, 1999, **75**, 1679.

20 C.-C. Wu, Y.-T. Lin, K.-T. Wong, R.-T. Chen and Y.-Y. Chien, *Adv. Mater.*, 2004, **16**, 61.

21 J. Y. Shih, C. Y. Lee, T.-H. Huang, J. T. Lin, Y.-T. Tao, C.-H. Chien and C. Tsia, *J. Mater. Chem.*, 2005, **15**, 2455.

This journal is © The Royal Society of Chemistry 2009

J. Mater. Chem., 2009, **19**, 1865–1871 | 1871